J. Membrane Biol. 208, 103–111 (2005)
DOI: 10.1007/s00232-005-0823-y

The Journal of
Membrane
Biology

© Springer Science+Business Media, Inc. 2006

Wavelength- and Time-Dependence of Potentiometric Non-linear Optical Signals from Styryl Dyes

A.C. Millard, L. Jin[†], J.P. Wuskell, D.M. Boudreau[‡], A. Lewis, L.M. Loew
Center for Cell Analysis and Modeling, University of Connecticut Health Center, Farmington, CT 06030, USA

Received: 12 December 2005

Abstract. Second harmonic generation (SHG) imaging microscopy is an important emerging technique for biological research, complementing existing one- and two-photon fluorescence (2PF) methods. A non-linear phenomenon employing light from mode-locked Ti:sapphire or fiber-based lasers, SHG results in intrinsic optical sectioning without the need for a confocal aperture. Furthermore, as a second-order process SHG is confined to loci lacking a center of symmetry, a constraint that is readily satisfied by lipid membranes with only one leaflet stained by a dye. Of particular interest is ''resonance-enhanced'' SHG from styryl dyes in cellular membranes and the possibility that SHG is sensitive to transmembrane potential. We have previously confirmed this, using simultaneous voltage-clamping and non-linear imaging of cells to find that SHG is up to four times more sensitive to potential than fluorescence. In this work, we have extended these results in two directions. First, with a range of wavelengths available from a mode-locked Ti:sapphire laser and a fiber-based laser, we have more fully investigated SHG and 2PF voltage-sensitivity from ANEP and ASTAP chromophores, obtaining SHG sensitivity spectra that are consistent with resonance enhancements. Second, we have modified our system to coordinate the application of voltage-clamp steps with non-linear image acquisition to more precisely characterize the time dependence of SHG and 2PF voltage sensitivity, finding that, at least for some dyes, SHG responds more slowly than fluorescence to changes in transmembrane potential.

[†]*Present address:* Department of Biomedical and Health Information Sciences, University of Illinois at Chicago, 1919 West Taylor Street MC-530, Chicago IL 60612-7249, USA
[‡]*Present address:* R.T. Vanderbilt Company, Inc., 30 Winfield Street, Norwalk, CT 06856-5150, USA
Correspondence to: L.M. Loew; email: les@volt.uchc.edu

Key words: Non-linear imaging — Resonance enhancement — Patch clamp — Voltage sensitivity — Transmembrane potential — Fluorescence

Introduction

Non-linear optical phenomena occur when high intensity light interacts with optical materials. The distinction from linear phenomena arises from the dependence of this interaction on the light intensity raised to a power greater than unity. Both second harmonic generation (SHG) and two-photon excitation fluorescence (2PF) are second-order optical processes occurring at high light intensities, typically using ultrashort pulses of near-infrared light. The use of 2PF and SHG as novel mechanisms for achieving contrast in microscopy was first suggested by Sheppard and colleagues (Sheppard et al., 1977; Wilson & Sheppard, 1984). The advent of readily available femtosecond lasers and the maturation of laser scanning microscopy has made high resolution non-linear microscopy practical, even leading to commercial instrumentation (So et al., 2000; Campagnola & Loew, 2003; Millard et al., 2003a; Zipfel, Williams & Webb, 2003). Since 2PF and SHG are non-linear processes, with signals depending on the square of the excitation intensity, sufficient power density may occur in a microscope only at the focal point, resulting in intrinsic three-dimensional optical sectioning without the need for (or loss of signal due to) a confocal aperture. However, while 2PF involves the near-simultaneous absorption of two photons, raising a fluorophore to an excited state, followed by relaxation and non-coherent emission, SHG is a nearly instantaneous process in which two photons are converted into a single photon of twice the energy, emitted coherently. Since fluorescent processes involve the retention of energy by the

fluorophore for a finite time, they may lead to collateral photodamage that typically accompanies conversion of the fluorophore to a triplet state resulting in the production of singlet oxygen. For SHG these problems are minimized, if not avoided altogether, though SHG is rarely unaccompanied by fluorescence or some other absorptive process; indeed, SHG can be enhanced if the second harmonic transition is in resonance with an electronic absorption band (Heinz et al., 1982).

There are other differences between the two phenomena that can best be appreciated by a brief theoretical discussion. In general, the polarizability of a material is a power series in applied electric field, the coefficients for each term being the material's susceptibilities. With time-varying electric fields, this gives rise to a range of non-linear phenomena, including SHG from biological sources (Freund, Deutsch & Sprecher, 1986; Huang, Chen & Lewis, 1989; Rasing et al., 1989; Campagnola et al., 2002) and from synthetic dyes (Bouevitch et al., 1993; Ben-Oren et al., 1996; Campagnola et al., 1999; Peleg et al., 1999), third harmonic generation (Tsang, 1995; Müller et al., 1998; Millard et al., 1999; Yelin et al., 1999) and multi-photon absorption (Göppert-Mayer, 1931; Shen, 1984; Denk, Strickler & Webb, 1990). 2PF arises linearly with the imaginary part of the third-order susceptibility (Shen, 1984) and hence depends linearly on the concentration of fluorophores (i.e., staining level for a dye); SHG arises quadratically from the second-order susceptibility (Shen, 1984; Boyd, 1992) and hence depends quadratically on the concentration of harmonophores (Verbiest et al., 1998; Moreaux, Sandre & Mertz, 2000). Additionally, SHG is confined to loci lacking a center of symmetry, such as mismatched interfaces (Shen, 1984). This finds immediate application in biology given the ubiquity of lipid bilayers and chiral protein assemblies: asymmetric staining of plasma membranes breaks inversion symmetry while SHG can be further enhanced through molecular chirality (Byers et al., 1994; Campagnola et al., 1999).

Our recent work has demonstrated that non-linear optical imaging of styryl dyes is a powerful technique with varied applications, including the investigation of lipid phases (Jin et al., 2005) and the visualization of the dynamics of membrane-vesicle fusion following fertilization of an ovum (Millard, Terasaki & Loew, 2005). The main point of interest, however, is the possibility of significant voltage-sensitivity, combining the advantages of the optical determination of transmembrane potential with those of non-linear imaging. For 2PF, the characteristics of the voltage-sensitivity should be similar to those of (linear) one-photon fluorescence (1PF), since in both cases emission results from the same excited state of the dye molecule; 2PF has some possible practical advantages given the excitation light's greater penetration depth and its low collateral photobleaching and photodamage in thick specimens. Significant work has been undertaken to characterize the voltage sensitivity of SHG from styryl dyes (Bouevitch et al., 1993; Ben-Oren et al., 1996; Millard et al., 2003b; Dombeck, Blanchard-Desce & Webb, 2004; Nemet, Nikolenko & Yuste, 2004; Dombeck et al., 2005). In particular, we have previously investigated the dependence on wavelength of the voltage-sensitivity of such dyes by patch-clamping stained neuroblastoma cells and recording 2PF and SHG images as a function of clamp voltage (Millard et al., 2004). The present work considers two areas requiring further study. First, we extend our earlier results to longer wavelengths and consider dyes with different styryl chromophores, confirming that the voltage-sensitivity of SHG from these dyes is indeed resonance-enhanced. Second, we investigate the time dependence of the voltage sensitivity of 2PF and SHG to determine if the responses are sufficiently rapid to detect action potentials for eventual application of this technology to multisite recording of neuronal activity.

Materials and Methods

For full details of our non-linear imaging microscope, we refer the reader to previously published descriptions (Millard et al., 2003a; Millard et al., 2004). Our current microscope combines a Fluoview (Olympus) scan-head and an Axiovert (Zeiss) inverted microscope constructed for multiple imaging methodologies, including wide-field and (one-photon excitation) fluorescence imaging as well as SHG and 2PF imaging. Our laser sources include a Mira (Coherent) Ti:sapphire laser and a Femtopower (Fianium) fiber laser operating at 1064 nm (Millard, Jin & Loew, 2005). For excitation, we routinely use an IR-Achroplan (Zeiss) 40×, 0.8 NA water-immersion objective, though for shorter wavelengths we also use an A-Plan (Zeiss) 40×, 0.65 NA air objective. Fluorescence is imaged (for linear imaging) or collected (for non-linear imaging) back through the excitation objective, while SHG is collected in the forward transmitted light direction by a condenser, either 0.8 NA or 0.55 NA (Zeiss). For optimal collection, the numerical aperture of the condenser should be at least $1/\sqrt{2}$ of the numerical aperture of the excitation objective (Moreaux et al., 2000, 2001), though in practice a condenser of slightly lower numerical aperture will often suffice. Since the wavelength of second harmonic light is precisely half that of the excitation light, the choice of filter for SHG imaging is greatly simplified and the primary concern is the blocking of the excitation light that is also transmitted through the sample as well as fluorescence that is emitted forwards.

For characterizing the voltage-sensitivity of SHG as a function of wavelength, we used a switching protocol as previously described (Millard et al., 2003a, 2004). For investigating the time dependence of the voltage sensitivity, we modified the synchronization of our scanning and electrophysiology systems, triggering a step waveform for the voltage clamp approximately halfway through the page scan, as shown in Fig. 1. Image series were taken with frames alternating between switched (e.g., $0 \rightarrow -75$ mV) and unswitched (0 mV throughout), and the unswitched images were used to normalize the switched.

To ensure that our detectors (Hamamatsu R3896 photomultiplier tube for 2PF detection and Hamamatsu H7421-40

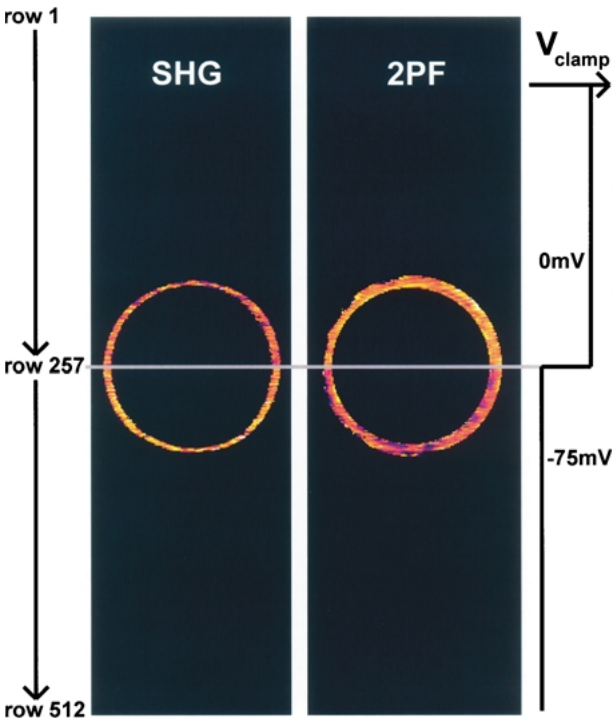

Fig. 1. To determine the time dependence of the voltage sensitivity of SHG and 2PF signals, the voltage clamp is synchronized to switch from 0 mV to −75 mV approximately half-way through a page-scan. Each row of the image takes 5 ms to acquire. The colors are mapped to intensities such that violet and blue represent lower signal levels and orange and yellow represent higher signal levels.

photon counting head for SHG) and Fluoview image acquisition did not introduce further time-dependent effects into these measurements, we used a uniform sample (actually a scale from a black tetra fish, *Gymnocorymbus ternetzi,* stained with di-8-ANEPPS, the collagen in the scale producing SHG and the dye producing 2PF) and synchronized a shutter such that it would open to allow the laser light to the scanning system approximately half-way through a page-scan. In this way, we verified that the SHG and 2PF signals both rose from a low background level to full intensity at the same instant when the shutter opened.

We used a variety of styryl dyes in this work, as shown in Fig. 2. Di-4-ANEPPS, Ebis(di-4-ANEP), di-4-ANEPPDHQ and di-6-ASPBS were synthesized by JPW and di-4-ASTAPPS was synthesized by DMB, using procedures adapted from Hassner et al. (Hassner, Birnbaum & Loew, 1984). Except for di-4-ANEPPDHQ, which is soluble in water, we prepared aqueous solutions of dye in complex with randomly carboxyethylated γ-cyclodextrin (Cyclodextrin Technologies) to facilitate and accelerate staining (Bullen & Loew, 2001; Millard et al., 2004; Wuskell et al., 2005).

Results

The wavelength dependence of the non-linear optical responses of di-4-ANEPPS to a 50 mV voltage step across the neuroblastoma cell membrane is shown in Fig. 3. Our previously published data for the SHG voltage-sensitivity (Millard et al., 2004) is included together with the newly acquired data for a wider

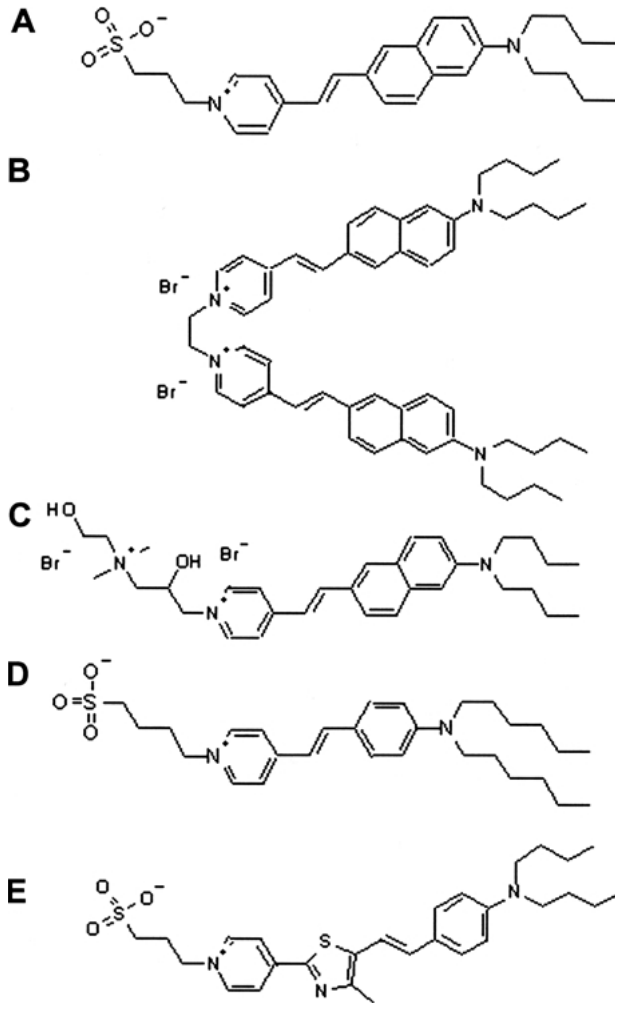

Fig. 2. Molecular structures of dyes used in this work. (*A*) di-4-ANEPPS. (*B*) Ebis(di-4-ANEP). (*C*) di-4-ANEPPDHQ. (*D*) di-6-ASPBS. (*E*) di-4-ASTAPPS.

range of wavelengths for both SHG and 2PF. Primarily for the SHG, we have extended the range of our measurement to 1064 nm by use of a femtosecond fiber laser in addition to the standard mode-locked Ti:sapphire laser. The additional data gives us confidence that the maximal sensitivity of the SHG signal, corresponding to ∼38% /100 mV (Millard et al., 2004), does occur in the 950 – 970 nm range. This corresponds to approximately twice the wavelength of the linear absorbance maximum of the dye bound to lipid vesicle membranes, ∼470 nm, suggesting a resonance phenomenon. In Fig. 3, we have also acquired two sets of 2PF data, "green" 2PF at 515 – 565 nm and "red" 2PF at 650 – 700 nm, corresponding to emission at the low and high wavelength wings of the emission spectrum, which has a maximum at ∼640 nm. The fluorescence response is similar to that observed for one-photon measurements (Fluhler, Burnham & Loew, 1985) as expected, being more negative at low wavelengths and more positive

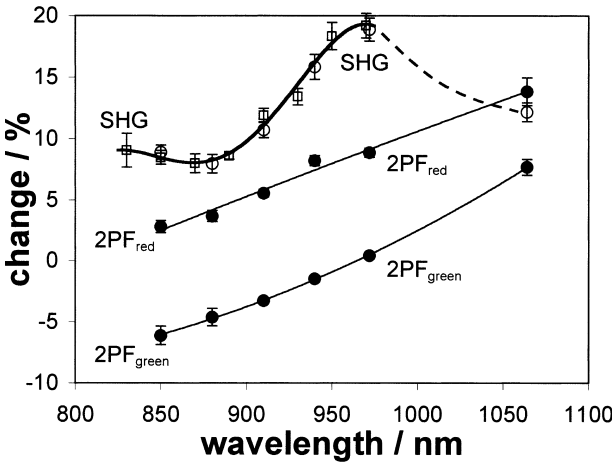

Fig. 3. Sensitivity spectra for SHG (*empty circles* and *squares*) and 2PF (*filled circles*) from di-4-ANEPPS for 0 → −50 mV, with data obtained from a total of fifty-five sets of measurements. Error bars show mean standard errors. *Empty squares*: SHG sensitivity data obtained in our earlier work (Millard et al., 2004). *Thick line*: simple fit demonstrating the trend of SHG sensitivity in the previous work. *Empty circles*: SHG sensitivity data obtained in this work, in agreement with the old data. *Dashed line*: simple extrapolation of the SHG sensitivity spectrum, given our new data at 1064 nm, consistent with resonance-enhancement. *Thin lines*: simple fits demonstrating trends in the sensitivity for "green" (515 – 565 nm) and "red" (650 – 700 nm) 2PF emission ranges as a function of excitation wavelength.

at high wavelengths. Notably, the red 2PF signal change for excitation at 1064 nm is 14% (corresponding to 28% /100 mV, as sensitivity is usually reported). This represents one of the largest sensitivities measured for fluorescence and is consistent with the idea that the voltage-sensitivity of an electrochromic dye is maximal at the spectral edge (Loew, 1982; Kuhn, Fromherz & Denk, 2004).

Table 1 lists sensitivity data for Ebis(di-4-ANEP) along with equivalent data for a new dye, di-4-ASTAPPS, which absorbs at the longer wavelength of ~525 nm and for which 2PF is detected at longer wavelengths. Interestingly, the SHG voltage-sensitivity for Ebis(di-4-ANEP) is larger at 1064 nm than at 972 nm, despite the fact that the latter wavelength is closer to twice the one-photon absorbance of 490 nm. This may originate from a hidden band at longer wavelengths due to a state-splitting interaction between the closely-spaced chromophores in this molecule (Fig. 2*B*). This new state may have a low extinction coefficient but a high two-photon cross section. The SHG of di-4-ASTAPPS was only measured at 1064 nm, corresponding to a near-resonance with twice the one-photon absorbance maximum. Although the sensitivities of both the SHG and the 2PF voltage-sensitivities are respectable, a more thorough exploration of their wavelength dependences remains to be performed to determine if these two dyes offer any improvement compared to di-4-ANEPPS.

We then examined the kinetics of the 2PF and SHG responses to a voltage step. Figure 4 shows the SHG signal (normalized and averaged over membrane pixels in each row) from di-4-ANEPPS excited at 916 nm for a 0 → −75 mV switch, using the protocol depicted in Fig. 1. The cell is held at 0 mV until the raster scan reaches the center of the cell at line 258, at which point the voltage is switched to −70 mV. While the SHG signal change of 14.5% is consistent with the sensitivity spectra shown in Fig. 3, the signal clearly takes a significant amount of time to change, and is fit to a single exponential with a time constant of 70.6 ms. By contrast, the 2PF signals have biphasic rapid and slow phases, as shown in Figs. 5 and 6. In both cases, there is an initial response that is instantaneous on the 5 ms timescale of this experiment, specifically a negative change for green 2PF (Fig. 5) and a positive change for red 2PF (Fig. 6). These rapid responses are followed in both cases by a slow rise that does not level off on the timescale of this experiment; importantly, the slow phase of the fluorescence change is much slower than the SHG response.

Another styryl dye, di-4-ANEPPDHQ, is of interest for its sensitivity to lipid phases and local cholesterol concentration (Jin et al., 2005) and, most relevantly, its successful application to multisite recording of membrane potential (Obaid et al., 2004). Its high solubility in water compared to di-4-ANEPPS makes it especially convenient for rapidly staining cells without resort to a vehicle such as DMSO or Pluronic F127. Figure 7 shows the SHG signal from di-4-ANEPPDHQ excited at 916 nm for a 0 → −100 mV switch. As was the case for di-4-ANEPPS (Fig. 4), the SHG signal does not change instantly. (Though these data are more noisy than those for di-4-ANEPPS, we have verified that our fitting algorithm is robust at such noise levels.) As was also the case for di-4-ANEPPS (Fig. 5), the green 2PF signal decreases instantly followed by a slow increase (Fig. 8).

Finally, di-6-ASPBS (Fluhler, Burnham & Loew, 1985) is a double-bonded analogue of DHPESBP, a styryl dye with a triple-bond linker between the two aromatic ring systems that has been used to study fast SHG changes in giant unilamellar vesicles (Moreaux et al., 2003) and in invertebrate neurons (Dombeck et al., 2004). Fig. 9 shows the SHG sign from di-6-ASPBS excited at 940 nm for a 0 → −100 mV switch. In this case the SHG signal change, if any, is at the same level as the noise and the fitted time constant, though large, is unreliable. As before, the green 2PF signal changes very quickly, in this case increasing, as shown in Fig. 10.

Discussion

We have presented results from two classes of experiments, the first determining the sensitivity of

Table 1. Sensitivity data for Ebis(di-4-ANEP) and di-4-ASTAPPs for 0 → −50 mV

	SHG		N	2PF		2PF	
Dye	Excitation	Change %		Emission range 1	Change %	Emission range 2	Change %
Ebis(di-4-ANEP)	972 nm	8.7 ± 1.3	6	515 – 565 nm	−4.3 ± 1.4	650 – 700 nm	2.5 ± 0.9
	1064nm	15.1 ± 0.3	5		−1.4 ± 0.5		6.4 ± 0.3
Di-4-ASTAPPS	1064 nm	13.3 ± 0.6	9	615 – 665 nm	0.6 ± 0.5	750 – 850 nm	6.2 ± 0.4

Uncertainties indicate mean standard errors given *N* sets of measurements.

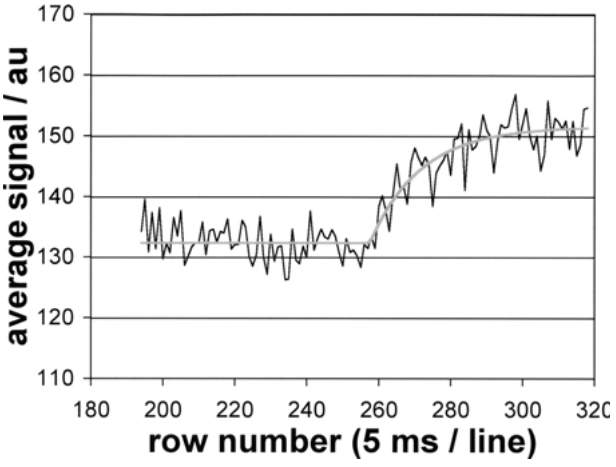

Fig. 4. SHG signal from di-4-ANEPPS excited at 916 nm for a 0 → −75 mV switch. The *black line* shows data obtained from, typically, 167 images (and as many as 215, depending on row number) while the *grey line* shows a fit (R = 0.94) based on an exponential rise to a final value, with τ = 70.6 ms and ΔS = 14.5%.

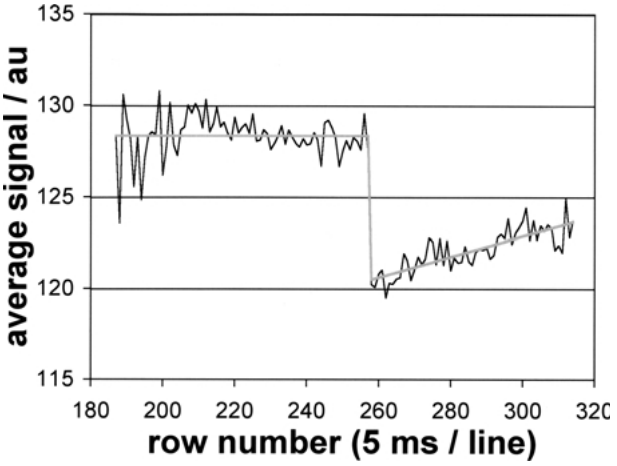

Fig. 5. Green 2PF (515 – 565 nm) signal obtained simultaneously with the data shown in Fig. 4. The *black line* shows data obtained from, typically, 112 images (and as many as 135, depending on row number) and the *grey line* shows a fit (R = 0.95) based on a step to an intermediate value (ΔS = −6.1%) followed by a linear rise at an initial rate of 9.3% s^{-1}.

SHG and 2PF from styryl dyes to trans-membrane potential at wavelengths out to 1064 nm and the second, investigating SHG and 2PF signal changes at millisecond timescales.

We extended our earlier work with di-4-ANEPPS (Millard et al., 2004) by measuring its SHG voltage-sensitivity at 1064 nm and increased the number of wavelengths investigated below 970 nm. We also fully characterized the 2PF voltage-sensitivity of this dye as a function of excitation wavelength with two emission bands corresponding to the long and short wavelength wings of the emission spectrum. Fig. 3 shows that the SHG sensitivity appears to peak around 970 nm, with a maximum of ~38% per 100 mV, which we previously assumed to arise from a two-photon resonance corresponding to the (one-photon) absorption peak at ~470 nm. Also, there is a difference in sensitivities for "red" 2PF (650 – 700 nm) and "green" 2PF (515 – 565 nm), and the sensitivity of the green 2PF changes sign in going from shorter to longer wavelengths. This biphasic response of the 2PF sensitivity is similar to that of 1PF (Fluhler, Burnham & Loew, 1985), consistent with

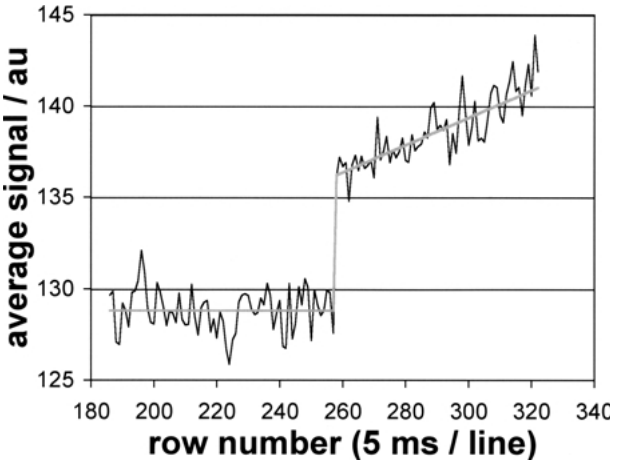

Fig. 6. Red 2PF (650 – 700 nm) signal obtained simultaneously with the data shown in Fig. 4. The *black line* shows data obtained from, typically, 57 images and the *grey line* shows a fit (R = 0.97) based on a step to an intermediate value (ΔS = 5.7%) followed by a linear rise at an initial rate of 11.0%s^{-1}

sensitivity arising from electrochromism (Loew et al., 1979; Loew, 1982, 1999). Notably, the sensitivity at 1064 nm for the red 2PF is ~28% / 100 mV, repre-

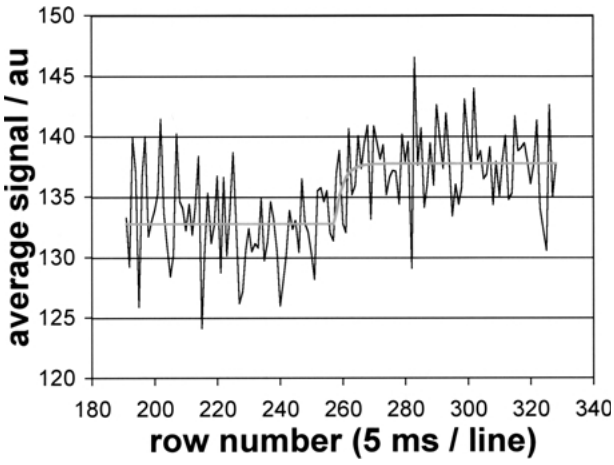

Fig. 7. SHG signal from di-4-ANEPPDHQ excited at 916 nm for a $0 \rightarrow -100$ mV switch The *black line* shows data obtained from, typically, 113 images (and as many as 130, depending on row number) while the *grey line* shows a fit ($R = 0.59$) based on an exponential rise to a final value, with $\tau = 12.2$ ms and $\Delta S = 3.8\%$.

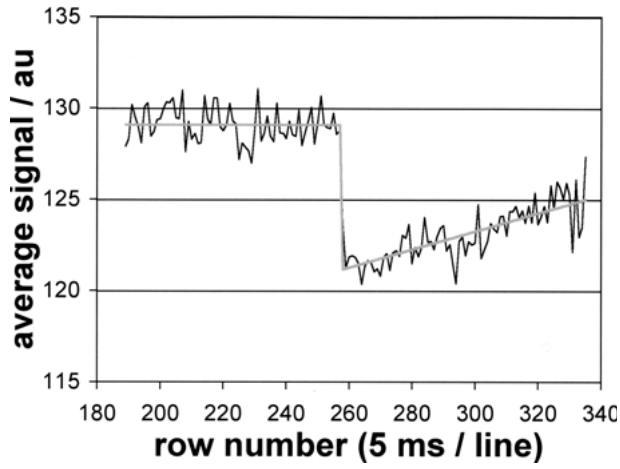

Fig. 8. Green 2PF signal obtained simultaneously with the data shown in Fig. 7. The *black line* shows data obtained from, typically, 117 images (and as many as 130, depending on row number) and the *grey line* shows a fit ($R = 0.96$) based on a step to an intermediate value ($\Delta S = -6.1\%$) followed by a linear rise at an initial rate of 8.2% s^{-1}.

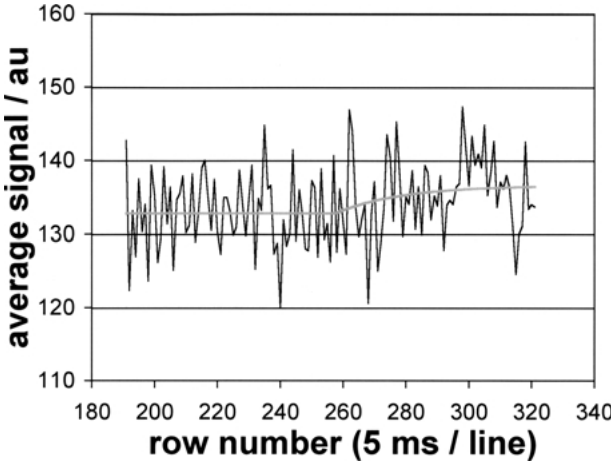

Fig. 9. SHG signal from di-6-ASPBS excited at 940 nm for a $0 \rightarrow -100$ mV switch. The black line shows data obtained from, typically, 59 images while the grey line shows a fit ($R = 0.27$) based on an exponential rise to a final value, with $\tau = 103.7$ ms and $\Delta S = 2.9\%$.

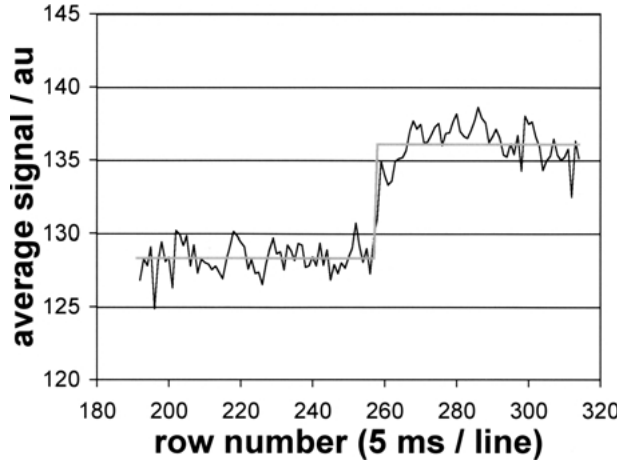

Fig. 10. Green 2PF signal obtained simultaneously with the data shown in Fig. 9. The *black line* shows data obtained from, typically, 65 images and the *grey line* shows a fit ($R = 0.94$) based on a simple step to a final value, with $\Delta S = 6.0\%$.

senting one of the largest sensitivities measured for fluorescence.

We have similarly measured sensitivities for two other dyes, allowing comparison with di-4-ANEPPS. Although two excitation wavelengths were probed, Table 1 suggests that there could be a shift of about 100 nm in going from the di-4-ANEPPS spectra to the data for Ebis(di-4-ANEP), consistent with a difference in their one-photon spectra of ~40 nm. Table 1 also shows that the sensitivity data for di-4-ASTAPPS at 1064 nm are comparable to those of di-4-ANEPPS at 930 nm, consistent with a one-photon absorption peak of ~525 nm compared with ~465 nm. Given its good sensitivity, combined with the greater penetration depth of laser light at 1064 nm, di-4-ASTAPPS is an attractive candidate for live tissue imaging.

While a good rule-of-thumb is that a material's two-photon spectrum may be obtained by doubling the wavelengths of the material's one-photon spectrum, the different quantum selection rules for the two processes mean that, even in the best cases, the correspondence is not exact (Xu et al., 1996). Here we have shown that the voltage-sensitivities of SHG from di-4-ANEPPS, Ebis(di-4-ANEP) and di-4-ASTAPPS depend on wavelength in ways that are consistent with two-photon resonances for which this rule-of-thumb holds reasonably well.

For applicability to neuroscience, where action potentials take place at millisecond timescales, the development of a class of "fast" probes for the optical imaging of transmembrane potential was a crucial development. The styryl dyes used in the present work are members of this class (Loew, 1999) and while such dyes have long been characterized and applied using 1PF (Loew et al., 1985, 1992; Wuskell et al., 2005), their application in SHG and 2PF imaging is a more recent development (Campagnola et al., 1999; Millard et al., 2004). Our previous work to characterize the voltage-sensitivity of SHG from these dyes used a slow switching protocol, and although the dependence of sensitivity on wavelength, as verified in this work, is consistent with a fast, resonance-enhanced mechanism, the dependence on time had not been measured directly.

Of the three dyes studied using the fast switching protocol described here, Fig. 9 shows that di-6-ASPBS does not exhibit any significant SHG voltage-sensitivity. Fig. 4 shows that while SHG from di-4-ANEPPS exhibited, as expected, a large sensitivity of ~20% / 100 mV at 916 nm, this took ~200 ms to achieve. Fig. 7 shows that SHG from di-4-ANEPPDHQ responded more quickly but with a smaller sensitivity, taking ~35 ms to achieve ~4% / 100 mV. These dyes, particularly di-4-ANEPPS, are known to be fast fluorescent probes (Loew, 1999) and we have confirmed that this is the case for 2PF. However, as Figs. 5 and 6 show for di-4-ANEPPS and Fig. 8 shows for di-4-ANEPPDHQ, after the initial, rapid change in 2PF signal, there follows an apparently linear increase in signal. A comparison between green 2PF (Fig. 6) and red 2PF (Fig. 5) shows that although the initial changes for these emission ranges are in opposite directions, the subsequent linear changes are in the same direction, reducing the net change for green 2PF and increasing the net change for red 2PF.

These results, taken together, indicate that changes in both SHG and 2PF signals do not simply result from a fast, electrochromic mechanism, and that in addition to a shift in electronic charge from the ground state to the first excited state, there may be an intramolecular rearrangement or a small movement of the dye molecule between chemical environments in response to an electric field. For instance, two-photon absorption is known to induce isomerization of di-6-ASPBS from the *trans*-form (Fig. 2D) to a *cis*-form with different physical and optical properties (Pons, Moreaux & Mertz, 2002) while the SHG voltage-sensitivity of di-6-APEQBS (which is not studied here) is known to depend on an electrochromic shift and a molecular realignment that are both induced on a sub-millisecond timescale (Pons et al., 2003).

Using the synchronized image scanning and voltage step protocol described in Fig. 1, the finite sizes of the cells prevent us from characterizing the long timescale kinetics of the changes in 2PF signal for di-4-ANEPPS and di-4-ANEPPDHQ, though the increases in signal must level out to some final value rather than continue to increase indefinitely. Nevertheless, we surmise that the 2PF signal changes may be the result of spectral shifts arising from either intramolecular rearrangements or molecular movements, small shifts in spectra manifesting as approximately linear changes in signal, as is the case for electrochromism (Fluhler, Burnham & Loew, 1985). Since such slow signal changes have not been reported for 1PF studies, they may, as in the case of the photo-isomerization of di-6-ASPBS, arise as a result of non-linear excitation. The SHG signal changes for di-4-ANEPPS and di-4-ANEPPDHQ are less readily interpreted, since they show a single component that is neither as fast as the initial fast change in 2PF nor as slow as the subsequent slow rises in 2PF signals. This implies that the SHG response results from a mechanism that is faster than the mechanism producing the slow component of the 2PF response and, while not simply electrochromic as was previously thought to be the case (Millard et al., 2003a), nevertheless depends on wavelength in a way that is consistent with two-photon resonance.

SHG voltage-sensitivity has generally been considered a fast "electro-optic" process that is analogous to the fast electrochromic response of fluorescence. Assuming that the only property of the system that is changing is the electric field, such as that corresponding to a cell's trans-membrane potential, SHG would arise from a combination of a purely second-order process and a third-order process dependent on that electric field. While this has been verified in non-biological systems for liquid/liquid (Conboy & Richmond, 1997) and solid/liquid (Yan, Liu & Eisenthal, 1998) interfaces, it is not clear how well this model applies in biological systems such as cellular membranes. An important complication is that dipole potentials from lipids and proteins produce electric fields near the membrane surface that may be as intense as 1 GV m^{-1} (Gross, Bedlack & Loew, 1994), significantly greater than the ~20 MV m^{-1} contribution of the transmembrane potential alone. It is known, for instance, that changes in dipole potential can be detected by 1PF imaging and spectroscopy (Bedlack et al., 1994; Gross, Bedlack & Loew, 1994; Xu & Loew, 2003), and we have performed some preliminary experiments (*results unpublished*) demonstrating that changes in dipole potential also affect SHG from styryl dyes in lipid membranes. Thus, it seems unreasonable to view an ~38% change in signal as a direct result of an ~2% change in the local electric field experienced by the individual dye molecules. The results we have presented here confirm that the contribution of the fast electro-optic process is not significant, suggesting that

changes in SHG from a cellular membrane are largely an indirect result of changes in trans-membrane potential. While the dye molecules may change shape, position or orientation under the influence of a local electric field, as discussed above, so may neighboring membrane molecules — it is known, for instance, that a change in transmembrane potential produces a change in the membrane's index of refraction, which can be understood in terms of a reorientation of dipoles (Stepnoski et al., 1991). Hence, the change in transmembrane potential may produce molecular rearrangements within the dye/membrane system that affect the second-order susceptibility, resulting in a change in SHG signal.

Finally, we should consider the implications of these results for the applicability of non-linear optics for recording electrical activity with sufficient sensitivity and temporal fidelity to be useful in neuroscience and cardiology. The 2PF signals are sufficiently fast to record neuronal action potentials and the sensitivity is at least as high as 1PF. Indeed the signal may be further enhanced in a dual-emission wavelength experiment where the ratio of red and green channels will provide a reduction in instrument noise and an increased change in response to potential. For SHG, however, the dyes tested here are too slow to faithfully record neuronal action potentials, even though the potentiometric sensitivity of at least one of them, di-4-ANEPPS, is outstanding. SHG from other styryl dyes has been shown to have sufficient speed to detect action potentials, albeit at a lower sensitivity (Moreaux et al., 2003; Dombeck, Blanchard-Desce & Webb, 2004; Dombeck et al., 2005). We shall continue to study the kinetics and optical characteristics of the 2PF and SHG responses of styryl dyes to transmembrane potential in order to develop dyes that provide high sensitivity at the millisecond timescale as would be required for a practical sensor of electrical activity in excitable cells and tissues.

In summary, we have extended our previous work by more systematically determining the SHG and 2PF voltage-sensitivities for di-4-ANEPPS at excitation wavelengths from 850 nm to 1064 nm, obtaining sensitivity spectra that are consistent with a two-photon resonance for SHG and biphasic responses for 2PF. The 2PF voltage-sensitivity of di-4-ANEPPS is especially high and could be of value for multisite recording of electrical activity from thick neuronal tissue. We have made similar measurements for Ebis(di-4-ANEP) and di-4-ASTAPPS, both of which absorb at longer wavelengths than di-4-ANEPPS and correspondingly have red-shifted sensitivity data. We have also developed a protocol for investigating the time dependence of the SHG and 2PF signals in response to step-like changes in transmembrane potential, finding that the SHG signals from di-4-ANEPPS and di-4-ANEPPDHQ take a significant amount of time to change, with time constants in tens of milliseconds and that the 2PF signals exhibit both initial, rapid changes and subsequent, slower changes. While we have made some comments regarding some possible mechanisms underlying these changes, further work needs to be undertaken to investigate these possibilities.

The authors are grateful to Lawrence P. Cunningham, Dr. Heather A. Clark, Dr. Nicholas Hernjak, Dr. James Watras, Dr. Mei-de Wei, Dr. Elizabeth L. Weitzke and Prof. Paul L. Campagnola for many helpful discussions and useful suggestions during the course of this work. ACM thanks Prof. Vladimir Rodionov for the fish scale. We gratefully acknowledge financial support under NIH grant GM35063.

References

Bedlack, R.S., Wei, M.-D., Fox, S.H., Gross, E., Loew, L.M. 1994. Distinct electric potentials in soma and neurite membranes. *Neuron* **13:**1187–1193

Ben-Oren, I., Peleg, G., Lewis, A., Minke, B., Loew, L.M. 1996. Infrared non-linear optical measurements of membrane potential in photoreceptor cells. *Biophys. J.* **71:**1616–1620

Bouevitch, O., Lewis, A., Pinevsky, I., Wuskell, J.P., Loew, L.M. 1993. Probing membrane potential with non-linear optics. *Biophys. J.* **65:**672–679

Boyd, R.W. 1992. Non-Linear Optics. Academic Press, San Diego

Bullen, A., Loew, L.M. 2001. Solubility and intracellular delivery of hydrophobic voltage-sensitive dyes with chemically-modified cyclodextrins. *Biophys. J.* **80:**168a

Byers, J.D., Lee, H.I., Petralli-Mallow, T., Hicks, J.M. 1994. Second harmonic generation circular dichroism spectroscopy from chiral monolayers. *Phys. Rev. B* **49:**14643–14647

Campagnola, P.J., Loew, L.M. 2003. Second harmonic imaging microscopy for visualizing biomolecular arrays in cells, tissues and organisms. *Nature Biotech.* **21:**1356–1360

Campagnola, P.J., Millard, A.C., Terasaki, M., Hoppe, P.E., Malone, C.J., Mohler, W.A. 2002. Three dimensional high resolution second harmonic generation imaging of endogenous structural proteins in biological tissues. *Biophys. J.* **82:**493–508

Campagnola, P.J., Wei, M.-D., Lewis, A., Loew, L.M. 1999. High resolution non-linear optical microscopy of living cells by second harmonic generation. *Biophys. J.* **77:**3341–3349

Conboy, J.C., Richmond, G.L. 1997. Examination of the electrochemical interface between two immiscible electrolyte solutions by second harmonic generation. *J. Phys. Chem. B* **101:**983–990

Denk, W., Strickler, J.H., Webb, W.W. 1990. Two-photon laser scanning fluorescence microscopy. *Science* **248:**73–76

Dombeck, D.A., Blanchard-Desce, M., Webb, W.W. 2004. Optical recording of action potentials with second-harmonic generation microscopy. *J. Neurosci.* **24:**999–1003

Dombeck, D.A., Sacconi, L., Blanchard-Desce, M., Webb, W.W. 2005. Optical recording of fast neuronal membrane potential transients in acute mammalian brain slices by second harmonic generation microscopy. J. Neurophysiol. 94: 3628–3636

Fluhler, E., Burnham, V.G., Loew, L.M. 1985. Spectra, membrane binding and potentiometric responses of new charge-shift probes. *Biochemistry* **24:**5749–5755

Freund, I., Deutsch, M., Sprecher, A. 1986. Connective tissue polarity. *Biophys. J.* **50:**693–712

Göppert-Mayer, M. 1931. über Elementarakte mit zwei Quantensprüngen. *Ann. Phys.* **9:**273–294

Gross, E., Bedlack, R.S., Loew, L.M. 1994. Dual-wavelength ratiometric fluorescence measurement of the membrane dipole potential. *Biophys. J.* **67:**208–216

Hassner, A., Birnbaum, D., Loew, L.M. 1984. Charge-shift probes of membrane, potential: synthesis. *J. Org. Chem.* **49:**2546–2551

Heinz, T.F., Chen, C.K., Ricard, D., Shen, Y.R. 1982. Spectroscopy of molecular monolayers by resonant second harmonic generation. *Phys. Rev. Lett.* **48:**478–481

Huang, J., Chen, Z., Lewis, A. 1989. Second harmonic generation in purple membrane poly(Vinyl Alcohol) films: Probing the dipolar characteristics of the bacteriorhodopsin chromophore in bR_{570} and M_{412}. *J. Phys. Chem.* **93:**3314–3320

Jin, L., Millard, A.C., Wuskell, J.P., Clark, H.A., Loew, L.M. 2005. Cholesterol-enriched lipid domains can be visualized by di-4-ANEPPDHQ with linear and non-linear optics. *Biophys. J.* **89:**L04–L06

Kuhn, B., Fromherz, P., Denk, W. 2004. High sensitivity of Stark-shift voltage-sensing dyes by one- or two photon excitation near the red spectral edge. *Biophys. J.* **87:**631–639

Loew, L.M. 1982. Design and characterization of electrochromic membrane probes. *J. Biochem. Biophys. Meth.* **6:**243–260

Loew, L.M. 1999. Potentiometric membrane dyes and imaging membrane potential in single cells. *In:* Manson, W.T., editor Fluorescent and Luminescent Probes for Biological Activity. pp 210–221, Academic Press, New York

Loew, L.M., Cohen, L.B., Dix, J., Fluhler, E.N., Montana, V., Salama, G., Wu, J.Y. 1992. A naphthyl analog of the aminostyryl pyridinium class of potentiometric membrane dyes shows consistenty sensitivity in a variety of tissue cell and model membrane preparations. *J. Membrane Biol.* **130:**1–10

Loew, L.M., Cohen, L.B., Salzberg, B.M., Obaid, A.L., Bezanilla, F. 1985. Charge shift-probe of membrane potential: Characterization of aminostyrylpyridinium dyes on the squid giant axon. *Biophys. J.* **47:**71–77

Loew, L.M., Scully, S., Simpson, L., Waggoner, A.S. 1979. Evidence for a charge-shift electrochromic mechanism in a probe of membrane potential. *Nature* **281:**497–499

Millard, A.C., Campagnola, P.J., Mohler, W., Lewis, A., Loew, L.M. 2003a. Second harmonic imaging microscopy. *Meth. Enzymol.* **361:**47–69

Millard, A.C., Jin, L., Lewis, A., Loew, L.M. 2003b. Direct measurement of the voltage sensitivity of second harmonic generation from a membrane dye in cells. *Opt. Lett.* **28:**1221–1223

Millard, A.C., Jin, L., Loew, L.M. 2005. Second harmonic generation imaging microscopy with a high power ultrafast fiber laser. *In:* Commercial and Biomedical Applications of Ultrafast Lasers. SPIE, San Jose, CA

Millard, A.C., Jin, L., Wei, M.-D., Wuskell, J.P., Lewis, A., Loew, L.M. 2004. Sensitivity of second harmonic generation from styryl dyes to transmembrane potential. *Biophys. J* **86:**1169–1176

Millard, A.C., Terasaki, M., Loew, L.M. 2005. Second harmonic imaging of exocytosis at fertilization. *Biophys. J.* **88:**L46–L48

Millard, A.C., Wiseman, P.W., Fittinghoff, D.N., Wilson, K.R., Squier, J.A., Muller, M. 1999. Third harmonic generation microscopy by use of a compact, femtosecond fiber laser source. *App. Opt.* **38:**7393–7397

Moreaux, L., Pons, T., Dambrin, V., Blanchard-Desce, M., Mertz, J. 2003. Electro-optic response of second harmonic generation membrane potential sensors. *Opt. Lett.* **28:**625–627

Moreaux, L., Sandre, O., Charpak, S., Blanchard-Desce, M., Mertz, J. 2001. Coherent scattering in multi-harmonic light microscopy. *Biophys. J.* **80:**1568–1574

Moreaux, L., Sandre, O., Mertz, J. 2000. Membrane imaging by second harmonic seneration microscopy. *J. Opt. Soc. Am. B* **17:**1685–1694

Müller, M., Squier, J.A., Wilson, K.R., Brakenhoff, G.J. 1998. Three-dimensional microscopy of transparent objects using third harmonic seneration. *J. Microsc.* **191:**266–274

Nemet, B.A., Nikolenko, V., Yuste, R. 2004. Second harmonic imaging of membrane potential of neurons with retinal. *J. Biomed. Opt.* **9:**873–881

Obaid, A.L., Loew, L.M., Wuskell, J.P., Salzberg, B.M. 2004. Novel naphthylstyryl-pyridinium potentiometric dyes offer advantages for neural network analysis. *Neurosci. Methods* **134:**179–190

Peleg, G., Lewis, A., Linial, M., Loew, L.M. 1999. Non-linear optical measurement of membrane potential around single molecules at selected cellular sites. *Proc. Nat. Acad. Sci. USA* **96:**6700–6704

Pons, T., Moreaux, L., Mertz, J. 2002. Photoinduced flip-flop of amphiphilic molecules in lipid bilayer membranes. *Phys. Rev. Lett.* **89:**288104-1–288104-4

Pons, T., Moreaux, L., Mongin, O., Blanchard-Desce, M., Mertz, J. 2003. Mechanisms of membrane potential sensing with second harmonic generation microscopy. *J. Biomed Opt.* **8:**428–431

Rasing, T., Huang, J., Lewis, A., Stehlin, T., Shen, Y.R. 1989. In situ determination of induced dipole moments of pure and membrane-bound retinal chromophores. *Phys. Rev. A* **40:**1684–1687

Shen, Y.R. 1984. The Principles of Non-Linear Optics. John Wiley & Sons, New York

Sheppard, C.J.R., Kompfner, R., Gannaway, J., Walsh, D. 1977. Scanning harmonic optical microscope. *IEEE J. Quantum Elect.* **13E:**100D

So, P.T.C., Dong, C.Y., Masters, B.R., Borland, K.M. 2000. Two photon excitation fluorescence microscopy. *Ann. Rev. Biomed. Eng.* **2:**399–429

Stepnoski, R.A., LaPorta, A., Raccuia-Behling, R, Blonder, G.E., Slusher, R.E., Kleinfeld, D. 1991. Non-invasive detection of changes in membrane potential in cultured neurons by light scattering. *Proc. Nat. Acad. Sci. USA* **88:**9382–9386

Tsang, T.Y.R. 1995. Optical third harmonic generation at interfaces. *Phys. Rev. A* **52:**4116–4125

Verbiest, T., Elshocht, S.V., Kauranen, M., Hellemans, L., Snauwaert, J., Nuckolls, C., Katz, T.J., Persoons, A. 1998. Strong enhancement of non-linear optical properties through supramolecular chirality. *Science* **282:**913–915

Wilson, T., Sheppard, C.J.R. 1984. Theory and Practice of Scanning Optical Microscopy. Academic Press, New York

Wuskell, J.P., Boudreau, D.M., Wei, M.-D., Jin, L., Engl, R., Chebolu, R., Bullen, A., Hoffacker K.D., Kerimo, J., Cohen, L.B., Zochowski, M.R., Loew, L.M. 2005. Synthesis, spectra, delivery and potentiometric responses of new styryl dyes with extended spectral ranges. *J. Neurosc. Meth.* in press

Xu, C., Loew, L.M. 2003. Activation of phospholipase C increases intramembrane electric fields in NlE-115 neuroblastoma cells. *Biophys. J.* **84:**4144–4156

Xu, C., Zipfel, W., Shear, J.B., Williams, R.M., Webb, W.W. 1996. Multiphoton fluorescence excitation: New spectral windows for biological non-linear microscopy. *Proc.Nat. Acad. Sci. USA* **93:**10763–10768

Yan, E.C.Y., Liu, Y., Eisenthal, K.B. 1998. New method for determination of surface potential of microscopic particles by second harmonic generation. *J. Phys. Chem. B.* **102:**6331–6336

Yelin, D., Silberberg, Y., Barad, Y., Patel, J.S. 1999. Phase matched third harmonic generation in a nematic liquid crystal. *Phys. Rev. Lett.* **82:**3046–3049

Zipfel, W.R., Williams, R.M., Webb, W.W. 2003. Non-linear magic: multiphoton microscopy in the Biosciences. *Nature Biotech.* **21:**1369–1377